High-Field Zeeman Anisotropy Fluorescence: Low-J Transitions of C_{4v}, C_s, and C_{2v} Sm^{2+} Sites in KCl†*

Francis K. Fong and James C. Bellows
Department of Chemistry, Purdue University, Lafayette, Indiana 47907
(Received 21 April 1970)

At 93.5 kG, all 23 observed 4.2 K fluorescence lines arising from the $^5D_0 \rightarrow {}^7F_0$, $^7F_1$, and $^7F_2$ transitions in KCl:Sm^{2+} show Zeeman effects, 11 of which give rise to Zeeman anisotropy fluorescence patterns. Contrary to the current postulate of a single complex model, it is shown that the fluorescence from these transitions actually arises from a mixture of (in the order of decreasing importance) C_{4v}, C_s, and C_{2v} sites. This finding lends strong support to the equilibrium distrubution theory of the Sm^{2+}-K^+ vacancy pairs.

I. INTRODUCTION

In recent investigations,[1,2] it has been shown that when divalent cations substitutionally enter the crystalline lattice of an alkali halide, their interactions with lattice cation vacancies at elevated temperatures[2] can be treated in terms of pair correlation functions of unit charges located at points in a periodic lattice, whereas at sufficiently low temperatures[1,2] the canonical configuration partition function reduces to a product of molecular pair partition functions from which an equilibrium distribution in M^{2+}-vacancy pair separations can be readily calculated.[1] The statistical mechanical considerations provided us with a satisfactory explanation of the initial Zeeman anisotropy fluorescence (ZAF) spectroscopic observation[3] of different site symmetries (tetragonal and orthorhombic) of Sm^{2+} ions in KCl. In addition, the statistical theory predicted[1] a large abundance of monoclinic sites corresponding to the hitherto unreported third nearest neighbor (nn) C_s (2, 1, 1) divalent cation-vacancy pair with the vacancy at the (2, 1, 1) lattice point. The importance of this monoclinic site has since been confirmed[4] by means of high-resolution ZAF investigations into the $^5D_0 \rightarrow {}^7F_3$ transition of KCl: Sm^{2+}. The application of the equilibrium distribution theory to trivalent cations in alkaline-earth halides has similarly led to the discovery of the monoclinic third nn M^{3+}-F^- interstitial pair in the CaF_2: U^{3+} system.[5]

All the ZAF determinations[3,4,6] thus far have been carried out at relatively low field strengths (~26 kG). Although most of the dominant fluorescence lines corresponding to $J \geq 3$ levels of KCl: Sm^{2+} [all of which arise from the $^5D_0 \rightarrow {}^7F_J$ ($0 \rightarrow J$) transitions[7]] give rise to ZAF patterns which have been analyzed to give definitive assignments of the site origins of the corresponding no-field lines, the lines arising from the $^5D_0 \rightarrow {}^7F_0$, $^7F_1$, and $^7F_2$ ($0 \rightarrow 0$, 1, and 2) transitions do not show detectable Zeeman shifts at 27 kG.[3] All the dominant lines in these transitions have been attributed by Bron and Heller[8] to Stark components of the nn C_{2v} Sm^{2+}-K^+ vacancy pair. By an indirect argument in terms of calculations including external magnetic fields,[3] it has been shown that the Bron-Heller[8] assignment appeared to be erroneous. Nevertheless, because of the lack of Zeeman shifts at the fields employed, the nn C_{2v} origin of the low-J lines was not refuted. Instead, the approximately even spacings of the major $0 \rightarrow 1$ and $0 \rightarrow 2$ lines have led to the possibility[9] of the vibronic origin of some of these lines. In the absence of definitive site origin determinations such as those afforded by the ZAF determinations, the earlier interpretations remain feasible speculations. However, according to the statistical theory,[1] the second nn C_{4v} (2, 0, 0) site, instead of the nn C_{2v} (1, 1, 0) site [which is even less important than the third nn C_s (2, 1, 1) site], is by far the most important. An assignment of all the major $0 \rightarrow 0$, 1, and 2 lines to the C_{2v} (1, 1, 0) site would thus appear contradictory to the distribution calculations.[1] It now seems more reasonable to expect, in view of the recent findings,[1-7] that the low-J lines, similar to what has been established for lines arising from the higher-J levels, should also exhibit a multiplicity of site origins characteristic of the compensated lattice problem. This problem can be readily resolved if we could reach some magnetic field strength at which the anisotropic Zeeman behavior of the various sites involved in the $0 \rightarrow 0$, 1, and 2 transitions can be detected.

In the present investigation, we shall extend the ZAF determinations of the $0 \rightarrow 0$, 1, and 2 lines to an external magnetic field of 93.5 kG. As a result of this investigation, it will be shown that, in agreement with the distribution calculations,[1] the observed fluorescence in question actually arises

from a mixture of (in the order of decreasing importance) C_{4v}, C_s, and C_{2v} sites. These results lead to a discussion of the larger problem of site distribution of divalent cations in *different* alkali halides in which the relative abundance of the C_{4v} (2, 0, 0) and C_{2v} (1, 1, 0) sites may reverse in importance depending on the ionic radius of the alkali-metalion. The discussion shall be concluded with the finding of empirical ΔJ selection rules in Sm^{2+}-vacancy pairs which depend, in a striking manner, on the site symmetry of the Sm^{2+} ion.

II. EXPERIMENTAL METHOD

KCl crystals containing 3.6×10^{18} Sm^{2+} ions cm^{-3} were grown by the Czochralski method.[10] The rare-earth content was determined by an ethylene diammine tetracetic acid (EDTA) analysis. The 4.2 K spectra were recorded on Kodak photographic N plates with a 2-m Bausch & Lomb grating (4×4 in., 15 000 per in.) spectrograph. The dispersions were 3.946, 3.787, and 3.748 Å/mm in the 0→0, 0→1, and 0→2 transition wavelength regions, respectively. A field of 93.5 kG was employed in the experiments which were carried out at the Francis Bitter National Magnet Laboratory (NML). Because an optical access perpendicular to the magnetic field was necessary, the maximum field (~215 kG) available at the NML was not utilized. The Zeeman fluorescence lines were calibrated by KCl:Sm^{2+} no-field spectra, which were in turn calibrated by means of an iron arc. The spectral lines were read with a Grant densitometer coupled to a Daytex programmer with digital output. The results were reproducible to an average deviation of 0.1 Å in most cases. The ZAF patterns were obtained with the magnetic field rotated in the (001) plane.

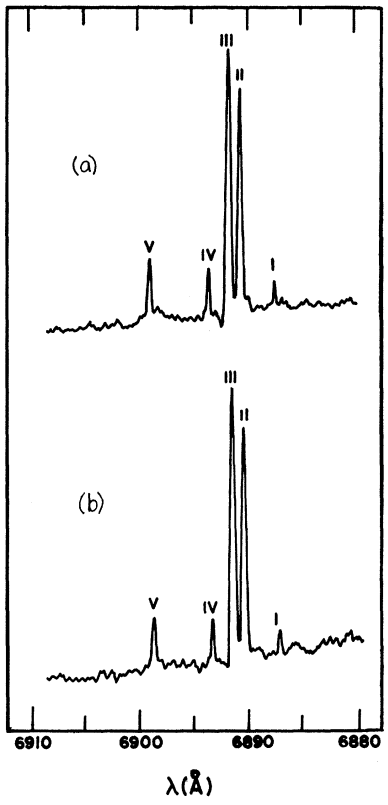

FIG. 1. 4.2 K fluorescence lines in the $^5D_0\rightarrow{}^7F_0$ transition region: (a) no field, (b) $\hat{H}$ (93.5kG) ‖[100].

TABLE I. Wavelengths, wave numbers, symmetry origins, and Zeeman shifts of the 23 observed 4.2 K lines in the 0→0, 0→1, and 0→2 transitions.

Transitions		λ(Å)	cm^{-1}	Symmetry origin	Zeeman shift (cm^{-1})
0→0	I	6887.6	14 518.9		+0.16
	II	6890.7	14 512.3		+0.10
	III	6891.9	14 509.8		+0.25
	IV	6893.8	14 505.8		+0.49
	V	6899.1	14 494.6		+0.35
0→1	VI	7014.7	14 225.8	C_{2v}	
	VII	7015.3	14 254.6	...	
	VIII	7018.0	14 249.1	C_s	
	IX	7018.8	14 247.5	...	
	X	7022.7	14 239.5	C_s	
	XI	7031.7	14 221.3	C_s	
	XII	7048.2	14 188.0		−0.08
0→2	XIII	7258.0	13 777.9	C_{4v}	
	XIV	7263.2	13 768.0	C_s	
	XV	7264.4	13 765.8	C_{2v}	
	XVI	7282.8	13 731.0	C_{4v}	
	XVII	7284.8	13 727.2	C_{4v}	
	XVIII	7286.0	13 725.0	...	
	XIX	7300.9	13 698.6	C_{4v}	
	XX	7304.6	13 690.0	C_{4v}	
	XXI	7320.8	13 659.7	...	
	XXII	7322.7	13 656.2	...	
	XXIII	7327.8	13 646.7		−1.22

III. EXPERIMENTAL RESULTS AND INTERPRETATIONS

The observed 4.2 K fluoresence lines I–XXIII in the 6887–7330 Å region are listed in Table I. In addition to the fact that there are many more lines than previously reported, the intense line at 6991.9 Å, which was thought to be a singlet due to insufficient resolution,[3,8] is in fact composed of two strong lines. The densitometer traces of the 23 observed no-field 0→0, 1, and 2 lines are shown in Figs. 1(a), 2(a), and 3(a). The corresponding lines under an external magnetic field of 93.5 kG with $\hat{H}$ ‖ [100] are shown in Figs. 1(b), 2(b), and 3(b), where it is shown that the no-field lines VI, VIII, X, XI, XIII–XVII, XIX, and XX each splits into two components while all the lines in 0→0 and the diffuse lines, VII and XXIII, exhibit no detectable Zeeman effect other than slight shifts in ener-

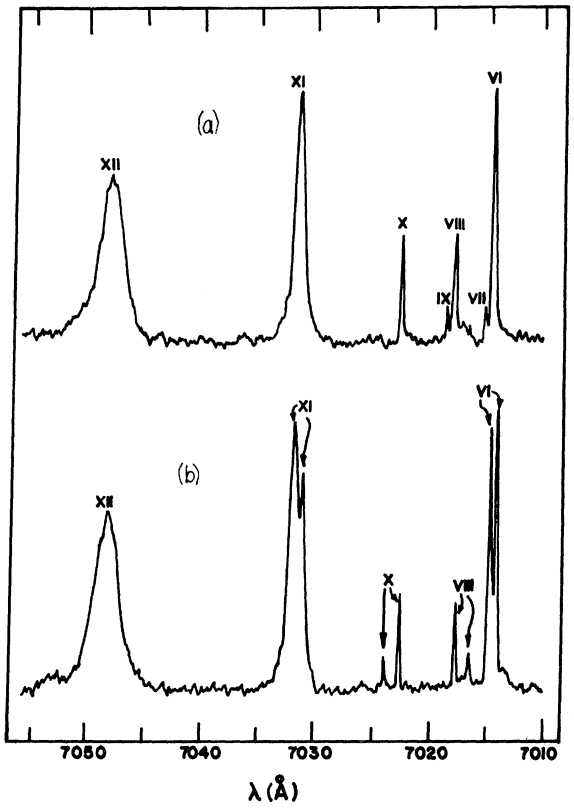

FIG. 2. 4.2 K fluorescence lines (VI–XII) in the $^5D_0 \rightarrow {}^7F_1$ transition region: (a) no field, (b) $\hat{H}$ (93.5 kG) $\parallel$ [100].

gy. These Zeeman shifts are isotropic, and are shown in wave numbers in Table I. The Zeeman components of VI, VIII, X, XI XIII–XVII, XIX, and XX give rise to discernible ZAF patterns as $\hat{H}$ is rotated in the (001) plane at intervals of $7\frac{1}{2}°$ from the [100] axis. The observed patterns are shown in Figs. 4 and 5, and their symmetry origins are listed in Table I along with their corresponding no-field lines. The remaining no-field lines VII, IX, XVIII, XXI, and XXII all appear to show Zeeman splittings. However, the line intensities of the Zeeman components are too weak for their anisotropy patterns to be discernible.

There are in all five no-field lines I–V in the 0→0 transition region, which must correspond to five different sites. Under the external field, all the 0→0 lines exhibit small blue shifts (Table I). These shifts are due to the fact that the magnetic field $\hat{H}$, being a tensor of rank one, gives rise to nonvanishing matrix elements of the type[11] $\langle 0, 0|\mathcal{H}^M|1, 0\rangle$, $\langle 0, 0|\mathcal{H}^M|1, 1\rangle$, and $\langle 0, 0|\mathcal{H}^M|1, \bar{1}\rangle$, where $\mathcal{H}^M$ is the operator form of the magnetic field; $\langle 0, 0|$, $|1, 0\rangle$, $|1, 1\rangle$, and $|1, \bar{1}\rangle$ denote the crystal-field states $\langle f^6, \alpha, {}^7F, J=0, M=0|$, $|f^6, \alpha, {}^7F, J=1, M=0\rangle$, $|f^6, \alpha, {}^7F, J=1, M=1\rangle$, and $|f^6, \alpha, {}^7F, J=1, M=-1\rangle$, respectively. Here f^6 is the electronic configuration of the Sm^{2+} ion, and α denotes all the quantum numbers not specified explicitly. There will be nonvanishing matrix elements involving crystal states of higher-J levels arising from high-order crystal-field perturbation. Due to the much larger energy separations which appear in the denominator in the perturbation terms, however, these matrix elements connecting the higher $|J, M\rangle$ states are unimportant. It should therefore be feasible to determine the site origin of the five 0→0 lines if we know the crystal-field Hamiltonians of the various possible $Sm^{2+} - K^+$ vacancy pairs from the observed Zeeman energy shifts such as those listed in Table I. This remains a task for future investigation. It is a task of considerable numerical difficulty since a convincing and unique fit of experiment must involve not only the ZAF data of all the observed lines in the seven ^7F_J levels, but also the field dependence of the associated Zeeman components as well as their polarizations. An initial effort in this direction involving the tetragonal C_{4v} sites has been reported.[7]

For the no-field lines which give rise to ZAF patterns, the data can be analyzed in terms of the magnetic field perturbation Hamiltonian

$$\mathcal{H}^M = g_\lambda \mu_B H_0 \left[\cos\theta_H J_Z + \tfrac{1}{2}\sin\theta_H (e^{i\phi_H} J_- + e^{-i\phi_H} J_+)\right],$$

where μ_B is the Bohr magneton, g_λ is the Landé g factor, H_0 is the effective magnetic field strength, θ_H is the angle between the H field and the Z axis of the $Sm^{2+} - K^+$ vacancy pair, and ϕ_H is the corresponding azimuthal angle. In C_{2v}, Z is taken to be the C_2 axis along the [110] direction. In C_{4v}, Z is chosen to be the C_4 axis along the [100] direction. In C_s, Z is taken to be the axis $\perp$ to the reflection plane. Detailed analyses of the ZAF patterns of these three symmetry types have been made in previous papers,[3,6] so that the patterns observed in the present work become immediately recognizable.

Of the no-field lines (VI, VIII, X, and XI) in the 0→1 transition region which show discernible ZAF patterns, only one (VI) is of C_{2v} origin. The remaining three lines are seen to be of C_s origin. They most probably arise from the three Stark states $(2A' + A'')$ of the $C_s(2, 1, 1)$ $Sm^{2+} - K^+$ vacancy pair. Of the seven no-field lines (XIII–XVII, XIX, and XX) in the 0→2 transition region which show discernible ZAF patterns, all but two (XIV and XV) are of C_{4v} origin. Since only two Zeeman components are observed for each of the five C_{4v} lines with $\hat{H} \parallel [100]$ [Fig. 3(b)], we first consider the possibility that all these lines arise from singlet transitions.[7] Under C_{4v} crystal field, $J=2$ decomposes into four crystal-field states: $A_1 + B_1 + B_2 + E$. Since the initial state is $^5D_0$, there

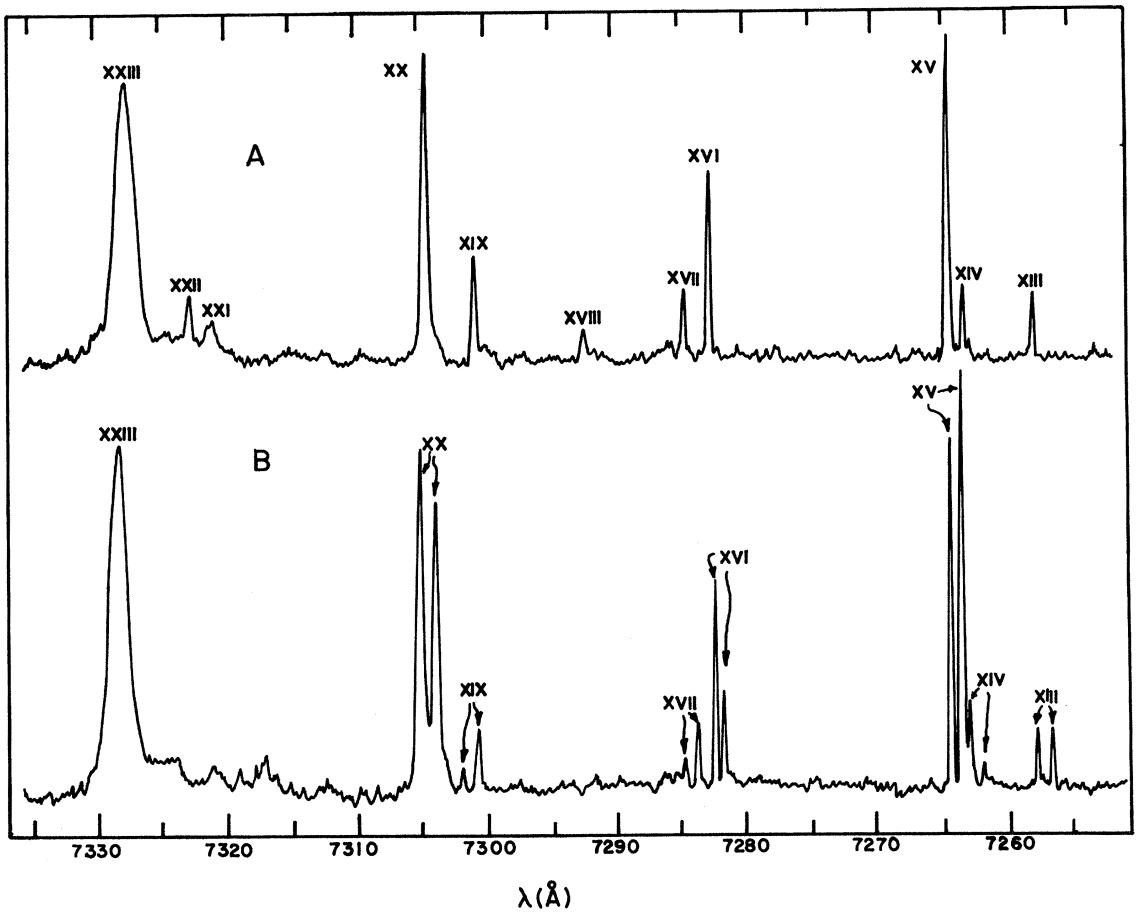

FIG. 3. 4.2 K fluorescence lines (XIII–XXIII) in the $^5D_0 \rightarrow {}^7F_2$ transition region: (a) no field, (b) $\hat{H}$ (93.5 kG) $\parallel$ [100].

should be a maximum of only one singlet transition of dipole origin $(0 \rightarrow A_1)$, if only one tetragonal site is present. If we exclude the role of quadrupolar transitions, which are very weak in rare earths, the observation of five singlet transitions must correspond to the presence of five *different* tetragonal sites. Even if we argue that lines XVII and XIX are doublet $(0 \rightarrow E)$ transitions, each with two of its four Zeeman components being too weak to be discernible or hidden by the much stronger components of lines XVI and XX, the remaining three singlet transitions XIII, XVI, and XX still point to the observation of at least three different tetragonal sites. It was shown,[7] in the discussion of the $0 \rightarrow 4$ tetragonal lines, that the two C_{4v} sites most likely responsible for the observed fluorescence are the C_{4v} (2, 0, 0) Sm^{2+}-K^+ vacancy pair and the C_{4v} (1, 0, 0) Sm^{2+}-O^{2-} pair. The observation of a third tetragonal site most probably means the detection of the eighth nn C_{4v} (4, 0, 0) Sm^{2+}-K^+ vacancy pair. On the basis of simple statistical considerations,[1,7] the relative probabilities of finding the C_{4v} (2, 0, 0) and C_{4v} (4, 0, 0) sites are, respectively, 7.7×10^{-1} and 1.1×10^{-4} at 300 K. The line intensities in Figs. 1–3 are recorded on a logarithmic scale. It is estimated that the intensity of the singlet line XIII is roughly 10^{-4}–10^{-5} that of line XX. The observation of the C_{4v} (4, 0, 0) site, therefore, does not appear to be inconsistent with our statistical calculations.

IV. DISCUSSION

The possible presence of O^{2-} compensation complicates the problem of site symmetry distribution calculation. However, as the O^{2-} ion concentration is expected to be small compared to the Sm^{2+} ion concentration, the method outlined[1] for the symmetry distributions of the Sm^{2+}-K^+ vacancy pairs should hold at least to a first approximation. That this is the case is supported by the observation that out of the 14 strong lines reported [3] for all the $^5D_0 \rightarrow 0, 1, 2, \ldots,$ 6 transition regions, there are 5, 3, and 2 lines of C_{4v}, C_s, and C_{2v} origins (see Table II), respectively, which is what we expect from our

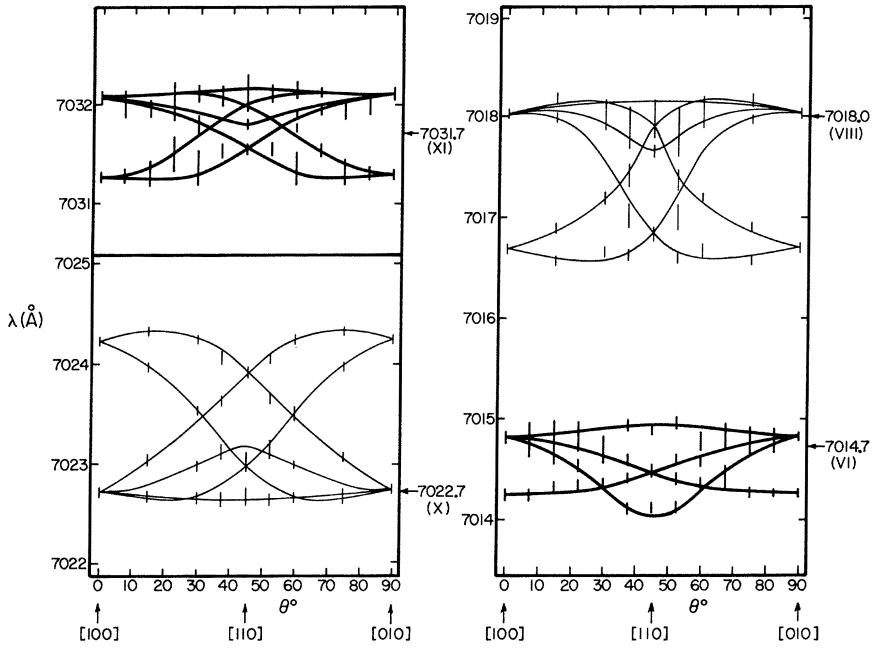

FIG. 4. High resolution C_{2v} (VI) and C_s (VIII, X, and XI) ZAF patterns observed for the ${}^5D_0 \rightarrow {}^7F_1$ transitions, with $\hat{H}$ rotated in the (001) plane. The pattern for XI is not well resolved.

statistical distribution calculations[1] in terms of the relative abundances of the $C_{4v}(2, 0, 0)$, $C_s(2, 1, 1)$, and $C_{2v}(1, 1, 0)$ divalent cation-vacancy pairs.

The fluorescence spectra[8] of KBr:Sm^{2+} and RbCl:Sm^{2+} are remarkably similar to the spectrum of KCl:Sm^{2+} reported here and elsewhere.[3,8] In fact, it is possible to attribute symmetry origins to most of the observed lines of Sm^{2+} in KBr and RbCl by virtue of their similarities (in terms of energy positions and relative intensities) to corresponding

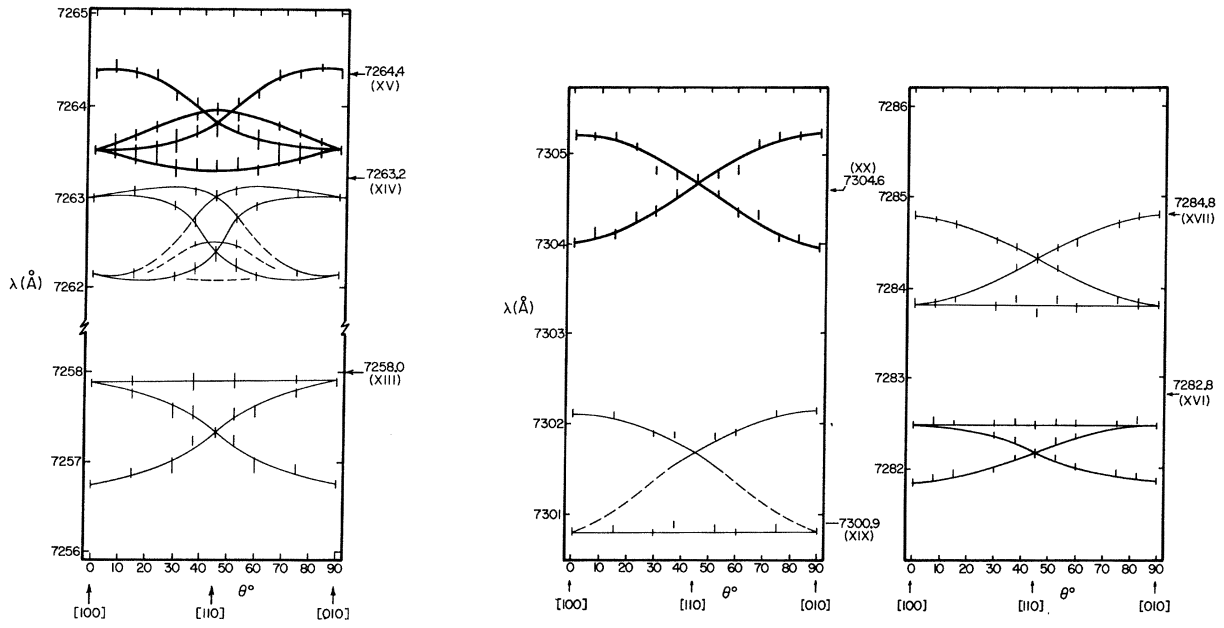

FIG. 5. High resolution C_{4v} (XIII, XVI, XVII, XIX, XX), C_{2v} (XV), and C_s (XIV) ZAF patterns observed for the $D_0 \rightarrow {}^7F_2$ transitions, with $\hat{H}$ rotated in the (001) plane. The patterns shown for XIV and XIX are tentative. Note that the isotropic component for the assigned C_{4v} pattern of XX is missing.

TABLE II. Dominant 4.2 K fluorescence lines in KCl : Sm^{2+} and their symmetry origins.

Transition	Wavelength	Symmetry	Reference
0 → 0	6891.9	?	
0 → 1	7014.7	C_{2v}	Present work
	7031.7	C_s	
	7048.2	?	
0 → 2	7264.4	C_{2v}	
	7282.8	C_{4v}	Present work
	7304.6	C_{4v}	
	7327.6	?	
0 → 3	7693.5	C_{3v}	4
	7694.5	C_s	4
0 → 4	8204.9	C_{4v}	3
0 → 5	8778.4	C_s	4
0 → 6	9439.1	C_{4v}	3
	9440.0	C_{4v}	

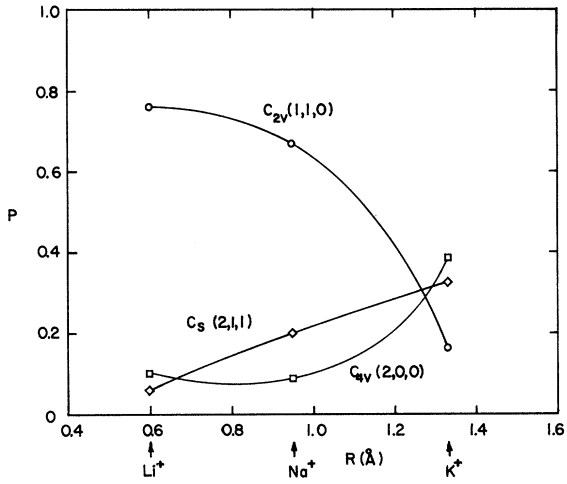

FIG. 6. Probabilities P of finding the C_{2v} (1, 1, 0), C_{4v}(2, 0, 0), and C_s(2, 1, 1) Mn^{2+}-cation vacancy pairs in LiCl, NaCl, and KCl at 300 K as a function of increasing host cationic radius.

lines in KCl: Sm^{2+} for which symmetry origins have been determined. The NaCl: Sm^{2+} system, on the other hand, gives rise to a very different spectrum[8] from that of KCl: Sm^{2+}. Clearly, a dramatically different distribution of site symmetries is responsible for this difference. Assuming the values − 0.45 and − 0.41 e V for ϵ_1 and ϵ_2, the first and second nn interaction energies,[12] respectively, for NaCl: Sm^{2+}, site distribution calculations actually show an overwhelming predominance of the C_{2v}(1, 1, 0) Sm^{2+}-Na^+ vacancy pairs over the C_{4v} (2, 0, 0) and C_s(1, 0, 0) pairs. The reversal in the relative importances of the nn and the second nn pairs as the ionic size of the host cation decreases is also manifested in the series of systems: LiCl: Mn^{2+} (ϵ_1 = − 0.3 eV, ϵ_2 = − 0.26 eV),[13] NaCl:Mn^{2+} (ϵ_1 = − 0.39 eV, ϵ_2 = − 0.35 eV),[13] and KCl:Mn^{2+} (ϵ_1 = − 0.39 eV, ϵ_2 = − 0.42 eV).[13] Distribution calculations give the probabilities P of finding the first three nn pairs, which are plotted as a function of the host cationic radius in Fig. 6. Again, the relative importances of the C_{4v} and C_{2v} sites reverse as the alkali-metal ion decreases in size. In their proposal of the single C_{2v}(1, 1, 0) nn complex theory for the (alkali halide) divalent rare-earth ion systems, Bron and Heller[8] omitted the NaCl: Sm^{2+} system because its fluorescence spectrum differs drastically from the spectra of the KCl: Sm^{2+}, KBr: Sm^{2+}, and RbCl: Sm^{2+} systems. As our own understanding of these compensated lattices develops, it becomes apparent that these authors have left out the only system for which the single C_{2v} (1, 1, 0) complex theory would have any meaning at all.

Finally, we wish to make several observations for the apparent ΔJ selection rules for the various symmetry types of Sm^{2+} sites. From Tables I and II, and from other earlier ZAF determinations, it is clear that (excepting the 0 → 0 transitions for which no definite site origin determinations are yet available) C_{4v} lines occur only in the 0 → 2, 4, and 6 (ΔJ even) transitions, C_s lines occur mostly in the 0 → 1, 3, and 5 (ΔJ odd) transitions, whereas C_{2v} lines occur mostly in the 0 → 1, and 2 transitions. From group-theoretical considerations, transitions from $^5D_0$ to *all* the lower ^7F_J levels are allowed. The peculiar ΔJ selection rules observed apparently arise for some subtle reasons which are not easily understood. They should serve as interesting material for future investigations.

†Research supported in part under the Advanced Research Project Agency, Grant No. SD102.

*The experimental work reported in this paper was carried out at the Francis Bitter Magnet Laboratory, Massachusetts Institute of Technology, Cambridge, Mass., which is supported by the Air Force Office of Scientific Research.

[1]F. K. Fong, Phys. Rev. 187, 1099 (1969).

[2]F. K. Fong, R. L. Ford, and R. H. Heist, Phys. Rev. (to be published).

[3]F. K. Fong and E. Y. Wong, Phys. Rev. 162, 348 (1967).

[4]F. K. Fong, Phys. Rev. B 1, 4157 (1970); F. K. Fong, M. N. Sundberg, R. H. Heist, and C. R. Chilver, *ibid.* (to be published).

[5]R. H. Heist and F. K. Fong, Phys. Rev. B 1, 2970 (1970).

[6]F. K. Fong, R. H. Heist, C. R. Chilver, J. C. Bellows, and R. L. Ford, J. Luminescence 1, 823 (1970).

[7]F. K. Fong and J. C. Bellows, Phys. Rev. B 1, 4240 (1970).

[8]W. E. Bron and W. R. Heller, Phys. Rev. 136, A1433 (1964).

[9]F. K. Fong and E. Y. Wong, in *Optical Properties of Ions in Crystals*, edited by H. M. Crosswhite and H. W. Moos (Interscience, New York, 1967), p. 137.

[10]F. K. Fong, J. A. Cape, and E. Y. Wong, Phys. Rev. 151, 299 (1966).

[11]M. Tinkham, *Group Theory and Quantum Mechanics* (McGraw-Hill, New York, 1964), Chap. 5.

[12]These values are actually calculated for the NaCl:Sr^{2+} system. F. Bassani and F. G. Fumi, Nuovo Cimento 11, 274 (1954); M. P. Tosi and G. Airoldi, *ibid.* 8, 584 (1958).

[13]G. D. Watkins, Phys. Rev. 113, 79 (1959); 113, 91 (1959).

PHYSICAL REVIEW B VOLUME 2, NUMBER 7 1 OCTOBER 1970

Behavior of Helical Spin Structures in Applied Magnetic Fields

J. M. Robinson and Paul Erdös

Department of Physics, The Florida State University, Tallahassee, Florida 32306

(Received 11 May 1970)

The problem of the behavior of helical spin structures and the phase transitions they exhibit in applied magnetic fields is studied theoretically. We have obtained a numerical solution valid for the planar helix at $T=0$ °K with an arbitrary number of interplanar exchange interactions, an arbitrary form of in-plane anisotropy, and an external magnetic field applied in the plane. We calculated the phase diagram for the case of two interplanar exchange constants and no anisotropy, and found different behavior in the intermediate field region from that predicted by the previous theory. As a new result, in the case of an in-plane anisotropy, the angle dependence of the transition fields has been obtained.

I. INTRODUCTION

A large number of materials are known, such as the rare-earth metals Tb,[1] Dy,[1] Ho,[1] Eu,[2] and the manganese compounds MnO_2,[3] $MnAu_2$,[4] and MnP,[5] which exhibit planar helical spin structures below the ordering temperature T_N. The model which is invoked to describe this situation is that of a succession of exchange-coupled ferromagnetic layers with the moment of a given layer lying in the plane of the layer. If the competing interlayer exchange constants are of sufficient magnitude, the classical ground state may be shown to be a spiral (helix), in which the angle between the magnetic moments of two consecutive layers is a constant q_0.

When an external magnetic field is applied parallel to the plane of the helix, transitions to other types of spin structures can be induced, resulting in discontinuities in the net magnetization and in the susceptibility. Nagamiya *et al.*[6] and Herpin *et al.*[7] have developed an approximate analytic theory for the planar spiral by series expansions. In weak fields the energy of the spin system is developed in powers of the applied field, assuming that the deviations of the spins from their directions in zero field are small. High field solutions are obtained by expanding the energy in powers of the angles of deviation of the spins from the field direction. The fields at which transitions between low and high field solutions, i.e., between two phases, occur were obtained by extending the curves which represent the energy as a function of the magnetic field to their intersection in intermediate fields. When there is anisotropy in the plane, this theory has been worked out in the special case of the magnetic field applied along a symmetry axis.[8] The preceding theory and its molecular field generalization to finite temperatures[8] have had wide application, but because of the approximations made, its validity for intermediate fields was not known. A more exact treatment is therefore needed.

We present here a numerical solution for a planar spiral at $T=0$ °K, whose axis of rotation is normal to the planes, with an arbitrary *in-plane anisotropy* and an *external field* applied in the plane at an arbitrary angle with respect to the in-plane anisotropy axes. The spins are assumed to be always constrained to the plane of the layers, as, for example, in the typical case of a strong